THE JOURNAL OF PHYSICAL CHEMISTRY C

Article

pubs.acs.org/JPCC

Kinetically Trapped Two-Component Self-Assembled Adlayer

Abdolreza Jahanbekam, Bhaskar Chilukuri, Ursula Mazur, and K. W. Hipps*

Department of Chemistry and Materials Science and Engineering Program, Washington State University, Pullman, Washington 99164-4630, United States

Supporting Information

ABSTRACT: A two-component self-assembly process that results in three different compositional phases is observed and explained. Solutions containing various molar ratios of cobalt octaethylporphyrin (CoOEP) and coronene in phenyloctane were brought into contact with a clean Au(111) surface. At no relative concentration was coexistence of the CoOEP and coronene phase observed. Rather, at intermediate concentrations a new 1−1 surface structure (1 coronene to 1 CoOEP) is formed with sharp compositional boundaries. This behavior is unusual in that only weak van der Waals forces, slight variations in surface charge exchange, and steric effects stabilize the 1−1 structure and that it occurs where the solution concentration ratio is an order of magnitude different than the surface concentration. The nature of this 1−1 structure and the transitions between the three phases (pure CoOEP, 1−1, and pure coronene) were studied by variable temperature STM and by density functional theory (DFT). Adsorption energies for CoOEP and coronene, both in their separate phases, and in the 1−1 structure were determined by DFT. The desorption energy into vacuum of CoOEP was found to be ∼1.8 times that of coronene, and the desorption energy of each component in the 1−1 composition was found to be greater than in the corresponding pure monolayer. Measured by energy per nm^2, pure CoOEP is predicted to be the most strongly adsorbed, coronene is predicted to be the least strongly adsorbed, and the 1−1 structure holds an intermediate position. By heating the sample to 50 °C it is possible to observe the transformation of the kinetically stabilized 1−1 structure into the pure CoOEP monolayer under the same solution from which it is formed at 22 °C. The existence of these three surface structures is shown to be a kinetic phenomenon rather than due to thermodynamics. We attribute the existence of the three structures at various growth concentrations to changes in nucleation and growth rate with relative impingement rates of each component. A critical element is the fact that one component (CoOEP) is irreversibly adsorbed. The new 1−1 structure is found to have lattice constants of A = (1.73 ± 0.04) nm, B = (1.56 ± 0.04) nm, and α = 90° ± 2° and appears to be commensurate with the Au(111) surface.

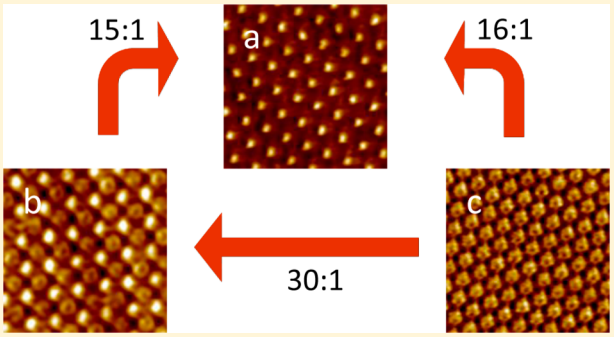

I. INTRODUCTION

The ability to design and build new molecular structures using molecular self-assembly is of utmost importance to the future of catalysis, sensing, and organic electronics.[1−7] An essential component of this rational design is the ability to both understand and to predict the surface structures that result from two-component adsorption processes. The difficulty in achieving such a general predictive understanding arises from the fact that the many participating forces are usually weak and are often only weakly directional.[8] van der Waals,[9] hydrogen bonding,[10] metal coordination,[11] dipole−dipole,[12] and substrate-mediated forces are all possible contributors. Initial demonstrations of the use of H-bonding, dipole−dipole forces, and metal coordination to produce new bimolecular monolayer phases were performed by vapor-depositing materials on metal substrates in UHV.[13−18] In these systems the creation of large-area uniform coverage depended on careful control of the material balance of the deposited components and often required annealing. The absence of exchange between the adsorbed phase and free molecules, the fact that many species of interest cannot be vapor-deposited, and the difficulty of controlling component concentrations over wide ranges are limitations of direct deposition methods.

Adsorption from the solution−solid interface allows the elimination of the above limitations. Often the same H-bonding and dipole−dipole forces that drive binary self-assembly in UHV are also seen at the solid−solution interface;[19−23] however, the process is significantly more complex than in UHV. In addition to the surface-molecular, intermolecular, and intramolecular interactions, the solvent also must be considered as it will certainly interact with the bare substrate, the solute, and the surface of the adlayer and can even be an integral part of the self-assembled layer.[24−27] Despite all of the complexity, the solution−solid interface is a very exciting environment to study. Solution−solid interface studies exemplify important biological environments[28] and are compatible with chemical equilibrium involving materials transport to and from the surface. In solution−solid studies, one can change the solvent

Received: July 22, 2015
Revised: October 6, 2015
Published: October 14, 2015

DOI: 10.1021/acs.jpcc.5b07120
J. Phys. Chem. C 2015, 119, 25364−25376

to tune molecule−solvent and substrate−solvent interactions, thereby changing the ordering and structure of the adsorbed species. The repair of defects in self-assembled layers at the solution−solid interface can be promoted if there is a dynamic exchange between molecules on the surface and in the solution phase. The cost and complexity of adlayer formation at the solution−solid interface is potentially much less than in UHV.

In general, upon introduction of a multicomponent solution onto the surface, several scenarios are possible. It can lead to phase segregation,[29−31] the formation of a randomly mixed monolayer (2-D solid solution not necessarily in equilibrium with the solution phase),[32,33] Langmuir-type adsorption where the surface concentration is proportional to the solution concentration,[32−35] preferential adsorption of one component,[35−38] or cocrystallization[8] on the surface. In addition, host−guest[39−44] structures are well known, bilayer[45] formation has been reported, and the use of surface potential in electrochemical cells has allowed construction of well-ordered binary structures.[36,46] In general, it is extremely unusual to see an abrupt transition from single-component adsorption to a monolayer of a bimolecular structure due to changes in concentration. A well-studied exception to this is the case of a binary fatty acid mixture studied by Flynn, where a sharp transition from single component to ordered dimer adsorption was observed as a function of concentration.[35] They attributed this to chemical equilibrium driven by a 1-D Ising model.

To study the complex variety of compositions and structures that can result at the solid−solution interface, scanning tunneling microscopy (STM) is unique in its ability to provide molecular-scale chemically sensitive images over a wide range of solution concentrations and temperatures.[47] Thus, most of our current knowledge of two-component self-assembly is the result of STM studies.

An understanding of the thermodynamics and kinetics at the solution−solid interface is essential to predict surface structures and their chemical and electronic properties. In fact, it is the competition between kinetics and thermodynamics that determines the driving force for making surface structures. The significance of this interplay between thermodynamics and kinetics was the topic of a 2015 review.[47] For quantitative evaluation of thermodynamic parameters one must be extremely cautious to make sure that the stable system is actually in dynamic equilibrium. For example, Friesen and coworkers[48] analyzed oxygen binding by cobalt octaethylporphyrin (CoOEP) at the phenyloctane/HOPG interface. They established through sequential imaging that it is in fact a dynamic equilibrium process. They were therefore able to use their STM measurements to calculate the enthalpy, entropy, and Gibbs free energy for the process. Stevens et al.,[49] using thiol molecules as markers in the STM image, demonstrated the existence of equilibrium between supernatant thiol/alcohol solution and thiol/alcohol monolayer on the surface. Blunt et al.[50] reported on polymorphism of alkylated dehydrobenzo[12]annulene (DBA) physisorbed at the 1,2,4-trichlorobenze/HOPG interface. They investigated the effect of temperature and concentration on the transition from a linear phase to a porous structure. Along with calculating the enthalpy and entropy for the transition, they identified the porous structure as the kinetically stable structure on the surface. On the contrary, there are examples in the literature that reveal that the formation of a given surface structure is kinetically controlled. Bhattarai et al.[32,33] showed that a two-component system of cobalt and nickel octaethylporphyrin at the phenyloctane-solution/Au(111) and at the phenyloctane-solution/HOPG interfaces produces a kinetically controlled randomly mixed monolayer on the surface. Schull et. al observed Arrhenius type hopping of coronene between host sites in an organic guest matrix.[42]

We explore competitive two-component adsorption of coronene and cobalt octaethylporphyrin (CoOEP) at the phenyloctane solution/Au(111) interface. By systematically changing the relative concentration of two components, we observe three different compositional phases on the surface. We show the existence of a pure CoOEP phase, a pure coronene phase, and a new cocrystallized structure having a unit cell containing one coronene and one CoOEP. At no concentration do we observed both CoOEP and coronene phases coexisting on the surface. By changing the relative concentration of two components, two sharp transitions between three phases were observed. We discuss the relative energies of the three stable phases with aid from periodic density functional theory (DFT) calculations. The competition between kinetics and thermodynamics for formation of the 1−1 coronene/CoOEP crystalline adlayer is considered. We also investigate the relative stability of each phase. We concluded that the new cocrystal structure is a kinetically trapped structure. This system is unusual in many ways, but the absence of any significant lateral forces other than van der Waals and steric constraints is notable. Also notable is the fact that the construction of the well-ordered 1−1 adlayer requires that the components have solution concentrations differing by a factor of >10.

II. EXPERIMENTAL METHODS

Coronene (99% pure) and 2,3,7,8,12,13,17,18-octaethyl-21*H*,23*H*-porphine cobalt(II) (CoOEP) were purchased from Aldrich and used as supplied. 1-Phenyloctane (98%) was purchased from Aldrich and was subjected to further purification, as described in the Supporting Information. Solubility of coronene in phenyloctane was measured from a saturated and filtered solution using an Evolution 260 Bio UV−vis spectrophotometer from Thermo Fischer. The solubility at 22 °C of coronene in phenyloctane was found to be 1.9×10^{-3} M. The solubility at 22 °C of CoOEP in phenyloctane is 2.6×10^{-4} M. Concentrations of coronene solutions used in this study ranged between (2.4 and 4.1) $\times 10^{-4}$ M, and the concentrations of CoOEP solutions were between 9.4×10^{-5} and 1.3×10^{-4} M. At all of these concentrations, either CoOEP alone or coronene alone will form a monolayer, and both are below their solubility limits. Mixed solutions of coronene and CoOEP were prepared by mixing appropriate volumes of stock solutions to make the desired relative molar concentrations. The total concentrations of mixed solutions were always below the solubility limits of each compound. The relative molar ratio ranged from 1.8:1 to 60:1 of coronene/CoOEP. In all reported relative molar ratios, the first number represents coronene and the second represents CoOEP. We also used solutions of pure CoOEP and of pure coronene. The solution compositions and relative ratios used are given in Table 1.

Vapor-deposited Au(111) films with well-defined terraces were epitaxially grown on mica.[51−53] Mica and Au (99.999% pure) were purchased from TedPella and Cerac, respectively. Deposited Au(111) substrates were ∼0.12 μm thick. The gold films were annealed with a hydrogen flame just prior to use. A home-built variable temperature solution-solid STM was used to image the samples.[54] The STM was controlled by a commercial Digital Instrument controller (now Bruker) and

DOI: 10.1021/acs.jpcc.5b07120
J. Phys. Chem. C 2015, 119, 25364−25376

Table 1. Concentrations Used (in mol/L) and Concentration Ratios

ratio ([coronone]/[CoOEP])	[coronene]	[CoOEP]
1.8	1.4×10^{-4}	7.8×10^{-5}
18	3.4×10^{-4}	1.9×10^{-5}
19	2.9×10^{-4}	1.5×10^{-5}
20	3.0×10^{-4}	1.5×10^{-5}
22	2.6×10^{-4}	1.2×10^{-5}
25	3.4×10^{-4}	1.4×10^{-5}
27	3.6×10^{-4}	1.4×10^{-5}
36	3.8×10^{-4}	1.1×10^{-5}
40	3.5×10^{-4}	8.7×10^{-6}
45	3.3×10^{-4}	7.5×10^{-6}
50	3.4×10^{-4}	6.7×10^{-6}
53	3.5×10^{-4}	6.7×10^{-6}
55	3.4×10^{-4}	6.2×10^{-6}
60	3.5×10^{-4}	5.9×10^{-6}

Nanoscope software. STM tips were made from annealed $Pt_{0.8}Ir_{0.2}$ purchased from California Fine Wire Company. Both etched and cut tips were used. STM samples were fabricated by placing a 20 μL droplet of solution directly on the gold surface. Typical settings were adjusted to give a sample bias of −700 mV, tunneling current of 50 pA, and a scan rate of 6.78 Hz. All STM images were background-subtracted using SPIP[55] image processing software. Drift correction of STM images has performed using a linear drift correction algorithm.[56,57] For surface coverage measurement, numerous good-quality images were analyzed at each molar ratio. Analysis was performed by first measuring the area of the minor surface structure and then subtracting that value from the total area. This was done for multiple images, and the results area was averaged to provide the final ratio of surface structures.

III. COMPUTATIONAL METHODS

All simulations were performed using the Vienna Ab Initio Simulation Package (VASP)[58−60] version 5.2. Periodic calculations were performed using plane-wave density functional theory (PW-DFT) within the projector-augmented wave (PAW) method[61,62] to describe the core electrons and valence−core interactions. On the basis of our experience on similar systems,[63] we found that dispersion DFT predicts the binding energies of organic species on surfaces relatively well in comparison with experiment. All calculations were performed with dispersion DFT using vdW-DF method,[64−66] which takes into account the nonlocal nature of electron correlation. The optB88-vdW GGA functional with PBE potentials having p, s semicore valence for Au and Co atoms was used. Calculations for isolated CoOEP and coronene molecules were carried out with similar functionals in conjunction with the respectively sized substrates. The choice of the DFT functionals was based on comparison of optimized lattice constant and bulk modulus[67] of *fcc*-gold unit cell with its crystal structure. The aforementioned functional was able to predict the geometries relatively well with <0.02 Å error in the lattice constant. For slab calculations, the electronic wave functions are sampled in a *k*-point grid of 2 × 2 × 1 for all systems in the irreducible Brillouin zone (BZ) using the Monkhorst and Pack (MP)[68] method. Isolated CoOEP and coronene molecules were sampled with only a gamma point. Plane-wave cut-off energy of 450 eV was used for all systems, and this value was determined from energy convergence tests on the respective primitive lattice. Methfessel−Paxton smearing was used to set the partial occupancies for each wave function with a smearing width of 0.2 eV.

IV. EXPERIMENTAL RESULTS AND DISCUSSION

On the basis of the relative molar concentration of coronene/CoOEP, three different structures at the phenyloctane/Au(111) interface were observed (Figure 1). These structures include the oblique structure of a pure CoOEP monolayer, the hexagonal structure of a pure high concentrations coronene adlayer, and a rectangular binary structure of the 1−1 structure formed from CoOEP and coronene. Exposure of Au(111) to a solution of pure CoOEP in phenyloctane resulted in the structure shown in Figure 1a. As expected, the cobalt center of the CoOEP appears high at the bias voltage used in this

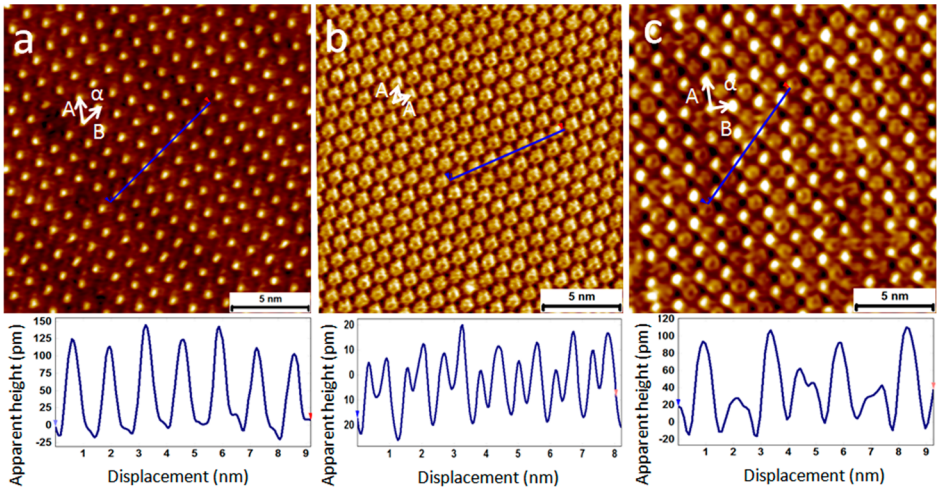

Figure 1. Three different surface structures on Au(111) at 22 °C based on relative molar concentration of coronene:CoOEP on Au(111). The unit cell for each structure is shown on each image. (a) CoOEP structure from pure CoOEP in phenyloctane at 9.8×10^{-5} M, A = (1.46 ± 0.04) nm, B = (1.34 ± 0.04) nm, and α = 56 ± 2° (b) coronene structure observed form pure coronene in phenyloctane at 3.0×10^{-4} M, A = (1.16 ± 0.04) nm. (c) Co-crystal of CoOEP and coronene formed at a 30:1 molar ratio of coronene to CoOEP in phenyl octane, A = (1.73 ± 0.04) nm, B = (1.56 ± 0.04) nm, and α = 90 ± 2°. Insets show line profiles of each structure.

DOI: 10.1021/acs.jpcc.5b07120
J. Phys. Chem. C 2015, 119, 25364−25376

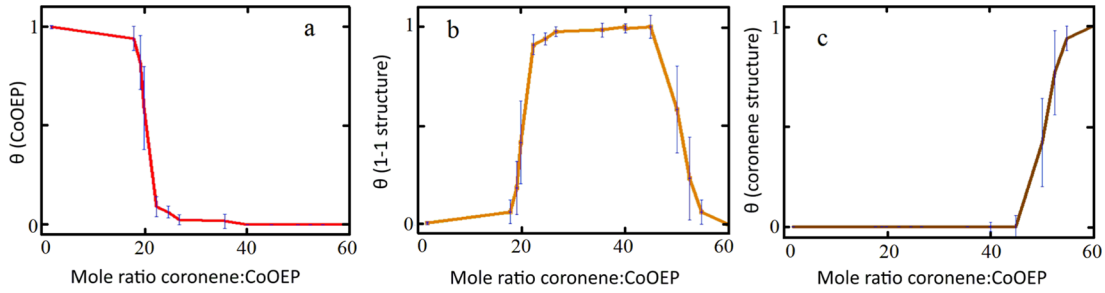

Figure 2. Surface coverage (θ) of three surface structures versus mole ratio of coronene:CoOEP in the solution. (a) Surface coverage of CoOEP structure versus mole ratio in solution. (b) Surface coverage of 1−1 structure versus mole ratio in solution. (c) Surface coverage of coronene structure vs mole ratio in solution.

study.[69,70] This can be observed in the cross section drawn in the inset of Figure 1a. A constant current STM image of the surface structure that occurs at the interface between Au(111) and coronene in phenyloctane solution is shown in Figure 1b. As can be seen in the cross section, coronene molecules show a depression in the center of each molecule. This difference between CoOEP and coronene clearly distinguishes these two molecules in STM images. Besides, as it is explained in the next paragraph, different unit cell parameters also allow the easy differentiation between phase-segregated structures of these molecules in STM images. Interestingly, exposing the gold surface to a mixture of CoOEP and coronene molecules did not result in phase segregation between coronene and CoOEP or in the formation of a solid solution on the surface. Instead a new cocrystal structure was formed at certain relative molar concentrations of the components in the mixture. This new structure is shown in Figure 1c. Phase segregation between pure CoOEP and the new structure at high CoOEP concentrations and between coronene and the new structure at extremely low CoOEP concentrations was observed only in very narrow regions of relative concentrations. CoOEP and coronene phases were never observed together. Eight representative surface images spanning the relative coronene/CoOEP range of 1.8:1 to 60:1 are shown in Figure S1.

Exposing clean Au(111) to a mixture of coronene:CoOEP up to a molar ratio of 18:1 in phenyl octane resulted in observing CoOEP as the main surface structure (Figure 1a). The unit cell defined in Figure 1a is assumed to have one molecule per unit cell, although it may actually be only half the true unit cell.[71] Upon increasing the relative concentration above 18:1, we observed an abrupt change in the resulting surface structure from pure CoOEP to a new cocrystal structure (Figure 1c). This new structure was composed of one coronene and one CoOEP molecule. We call this new structure the 1−1 structure. The 1−1 structure was the dominant structure on the surface until a relative molar concentration of 45:1. Beyond this ratio another sharp transition from 1 to 1 structure to a dense hexagonal coronene surface structure (Figure 1b) was observed. We previously reported on the existence of concentration-dependent polymorphism of adsorbed coronene at the heptanoic acid/Au(111) interface,[72,73] where three different concentration-dependent surface structures were seen. Although a different solvent is used in this current study (1-phenyloctane), it is important to mention that for the coronene concentration range used in this study ($(2.4 \text{ to } 4.1) \times 10^{-4}$ M), only the densely packed hexagonal structure was observed.

Figure 2 shows surface coverage of the three surface structures versus relative molar concentration in the solution. Figure 2a demonstrates that above the relative molar concentration of 18:1, the pure CoOEP structure did not occur on the surface. Figure 2b clearly shows the two sharp transitions from CoOEP structure to 1−1 structure and from 1 to 1 structure to coronene structure. It shows that the 1−1 structure is the dominant surface structure between 22:1 and 45:1 (coronene:CoOEP). Upon increasing the ratio to more than 55:1 only the coronene structure could be seen on the surface. Representative STM images of each surface structure along with STM images of transition regions are presented in Figure S1. It is extremely important to keep in mind that these structures were formed by exposing clean gold to a solution of the indicated relative concentration. As we shall see, changing the solution concentration after the monolayer formed did not necessarily yield the surface coverage one might predict from Figure 2.

To probe the role of kinetics in forming the above phases, we investigated the stability of each structure by first making one surface structure (by depositing a sample from the appropriate relative molar ratio solution), followed by adding a large excess of solution of different relative molar concentration on top of already-made surface structure. If one starts with the pure coronene structure on the surface and adds solution of 16:1 coronene/CoOEP (to form a final concetration of 16:1), the surface completely changes to the CoOEP structure expected at that relative concentration. On the contrary, starting with a surface covered with CoOEP structure followed by adding a solution of pure coronene on the surface, no change in the original CoOEP surface structure is observed. Even starting with the CoOEP structure resulting from contact with a 15:1 coronene/CoOEP molar ratio and flooding the sample with pure concentrated coronene solution did not make any change in the surface structure. The next experiment was to prepare a full monolayer of the CoOEP on the Au(111) structure formed from a 15:1 coronene/CoOEP solution. Then, a solution of 25:1 (which produces the 1−1 structure when added to clean gold) was added. This resulted in no change on the surface. Repeating the experiment in reverse by adding a solution having a 15:1 ratio on top of a formed 1−1 structure showed that the CoOEP structure replaced the 1−1 structure on the surface. These experiments indicate that the CoOEP structure, once formed on the surface, is inert to transitions to either 1−1 or pure coronene surface coverage.

To determine the relative adsorption strength of the 1−1 structure relative to the coronene structure, a solution of 30:1 ratio was added to a previously adsorbed coronene structure on Au(111). This caused the surface to quickly convert to the 1−1 structure. In the reverse experiment, a surface covered with the 1−1 structure (from a 40:1 molar ratio solution) was flooded with concentrated coronene. This produced no change in the

DOI: 10.1021/acs.jpcc.5b07120
J. Phys. Chem. C 2015, 119, 25364−25376

surface adlayer indicating that the 1−1 structure was resistant to conversion to coronene at room temperature. The results of these experiments are characterized in Figure 3, where transitions can only occur in the directions of the arrows.

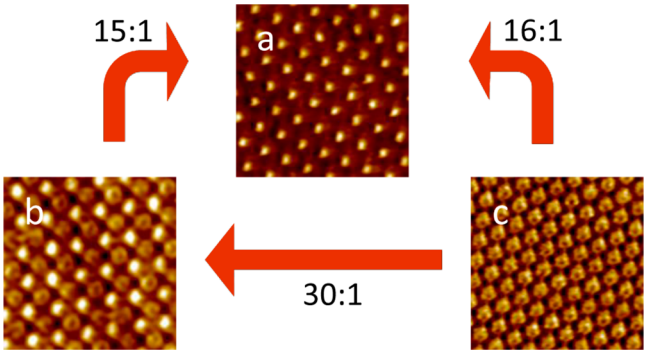

Figure 3. Changing the ratio of coronene to cobalt in the solution in contact with a given film structure could only drive the surface in one direction—toward the higher CoOEP phase. (a) CoOEP only, (b) 1−1 phase, and (c) pure coronene. The ratios given in the Figure are the coronene/CoOEP concentration ratios used to effect the conversions.

On the basis of the above observations, the formation of these surface phases is controlled by kinetics. If this system was at thermodynamic equilibrium, the forward steps in Figure 3 would be reversed by addition of a suitable concentration solution. They are not. Preferential adsorption of CoOEP below an 18:1 molar ratio suggests that CoOEP has a much greater binding energy on Au(111) relative to coronene and therefore a much slower desorption rate. This observation is consistent with our periodic DFT calculations (vide infra). Upon increasing the molar ratio above 18:1, we think that the rate of impingement of coronene on the substrate becomes competitive with the desorption rate, leading to the formation of the 1−1 structure. Growth of the 1−1 structure only makes sense based on preferential nucleation of the 1−1 phase at high coronene impingement rates, followed by growth that is faster than that of the CoOEP structure (at the relatively low impingement rates of the CoOEP). Increasing the relative concentration of coronene to CoOEP to more than 45:1 results in nucleation and growth of the coronene structure on the surface. It is necessary to mention that even at the relative molar ratio of 60:1 of coronene/CoOEP, in these experiments there were more than enough CoOEP molecules in the supernatant solution to make a monolayer of CoOEP on the surface.

Figure 4 shows a model for the 1−1 structure. It is apparent from the model that coronene and CoOEP molecules are very densely adsorbed on the surface. Itaya[74] showed a similar structure in which one zinc phthalocyanine molecule is surrounded by four zinc octaethylporphyrin molecules, where their suggested unit cell was a square. In this case, we have a structure made up of elements having 4- and 6-fold symmetry. The highest symmetry small unit cell that preserves the common two-fold axes is the rectangular one observed. Moreover, because the images appear uniform over large areas and because the lattice dimensions are consistent with a commensurate structure, our calculations are based on the commensurate structure, as shown in Figure 4.

There are a few reported studies that show similar surface bimolecular structures. They are predominantly seen in

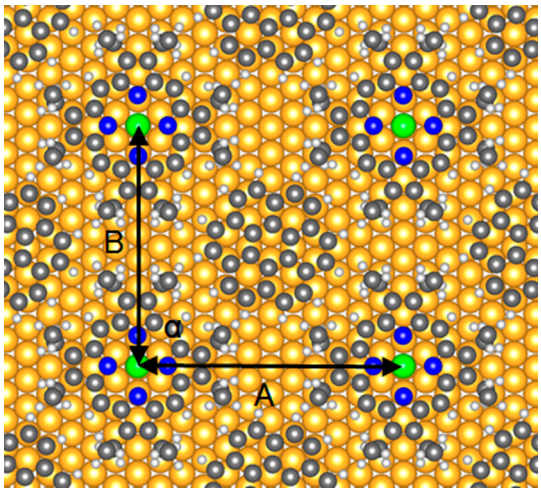

Figure 4. Molecular model of 1−1 structure, A = 1.73 nm, B = 1.56 nm, and α = 90°.

UHV[13−16] or in electrochemical environments.[20,74] In these reports, structures are either formed due to directing intermolecular forces, for example, hydrogen bonding, or they were made by manipulating the adsorption energy (via applied potential) to increase the rate of exchange of adsorbates between the surface and the solution; but, in the current 1−1 structure we do not see a possibility of hydrogen bonding between the species forming the cocrystal, and the experiment was performed under conditions where the desorption rate of CoOEP from the surface is extremely slow at room temperature (on the order of years).[32,33] As such, it can only be an interplay of van der Waals, dipolar, and steric forces between adsorbed molecules and strong adsorbate−substrate interactions stabilizing this unique 1−1 structure. We will delve more deeply into this in later sections.

While the kinetic stability of the CoOEP monolayer is well known, the stability of 1−1 structure is not and was investigated. In the course of 2 days at 22 °C, the 1−1 structure (made from and in contact with a 40:1 solution) did not show any conversion to other surface structures; however, in situ heating of the 1−1 structure to 50 °C induced conversion to the CoOEP structure. Figure 5 shows three images before heating, in the course of heating and after the heating. Figure 5a shows the surface before heating, which is completely covered by 1−1 structure. Figure 5b displays the surface at 50 °C and after 5.5 h of heating at 50 °C. For better comparison, in addition to drift correction, the image was corrected for scanner sensitivity alteration.[54] The sample was scanned also after returning to room temperature, as it is shown in Figure 5c. After 5.5 h at 50 °C, most of the surface has converted from the 1−1 structure to that of pure CoOEP. Once this conversion has occurred, cooling the sample to room temperature has no effect and the pure CoOEP layer is still present. (Note that the prominent vertical lines seen in Figure 5c are due to the underlying Au(111) reconstruction.) Consequently one can conclude that 1−1 structure is a kinetically favorable structure on the surface at room temperature in the molar ratio that is used; however, heating promotes more rapid desorption of coronene from the surface with preferential formation of the CoOEP structure. The fact that the 1−1 structure does not reappear on cooling verifies the fact that the CoOEP structure is actually a favorable structure

DOI: 10.1021/acs.jpcc.5b07120
J. Phys. Chem. C 2015, 119, 25364−25376

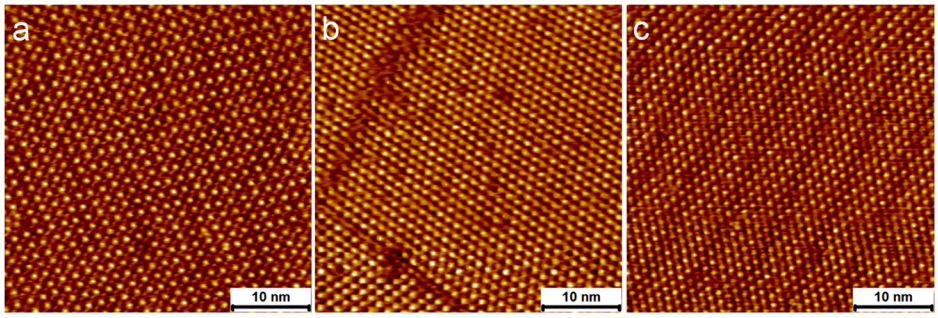

Figure 5. In situ heating of 1−1 structure. (a) 1−1 surface structure made from 40:1 solution. (b) In situ image of the same sample after 5.5 h at 50 °C showing CoOEP structure. (c) Same sample after coming back to room temperature showing CoOEP on the surface.

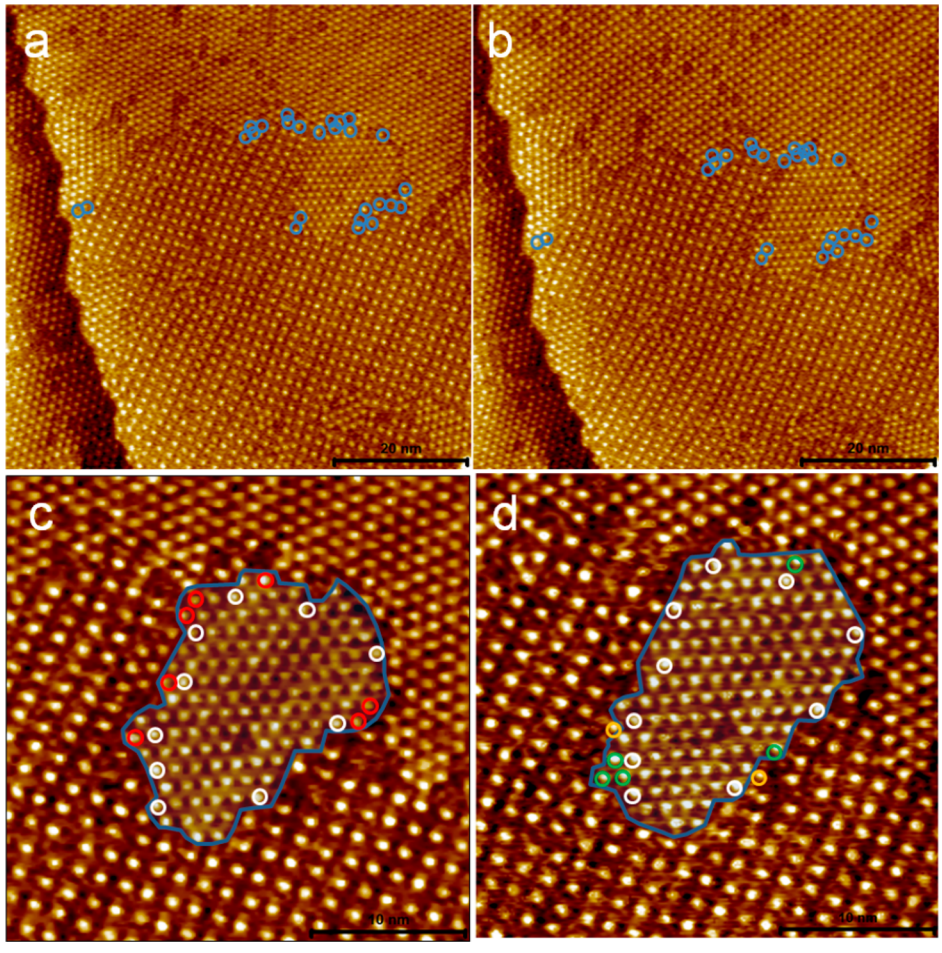

Figure 6. Tracking changes in two consecutive images at 22 °C. (a,b). Image a was captured before image b. The time interval is 75 s. Selected exchanging molecules are shown with blue circles. (c,d) Expanded images of the small central island in panels a and b, respectively. Red circles denote molecules lost from the ordered CoOEP island, green circles denote molecules added to the island, and the yellow circles identify selected molecules in disordered regions.

on the surface in the concentration range where the 1−1 structure is seen to form.

It should be noted here that the STM used was specifically designed for high-temperature studies of the solution−solid interface.[54] Even with a much more volatile solvent like toluene at temperatures as high as 75 °C, and periods as long as 24 h, no appreciable evaporation is observed. The boiling point of phenyloctane is 264 °C, while that of toluene is 111 °C. Thus, the changes seen in the adlayer are not simply concentration-dependent.

Time-dependent STM images were captured to determine the dynamic state of surface structures. Figure 6a,b shows two consecutive images of the surface formed at 22 °C from a 20:1 ratio solution. The coronene molecules that reside within the 1−1 domains remain unchanged over the 75 s time interval between images. At the grain boundaries, the low contrast and motion of the coronene makes it difficult to precisely identify them with time. Instead we focused on the CoOEPs, which were easily identified. In Figure 6, blue circles indicate CoOEP molecules that change position during the 75 s interval. The interchange of molecules at the solution/solid interface can

DOI: 10.1021/acs.jpcc.5b07120
J. Phys. Chem. C 2015, 119, 25364−25376

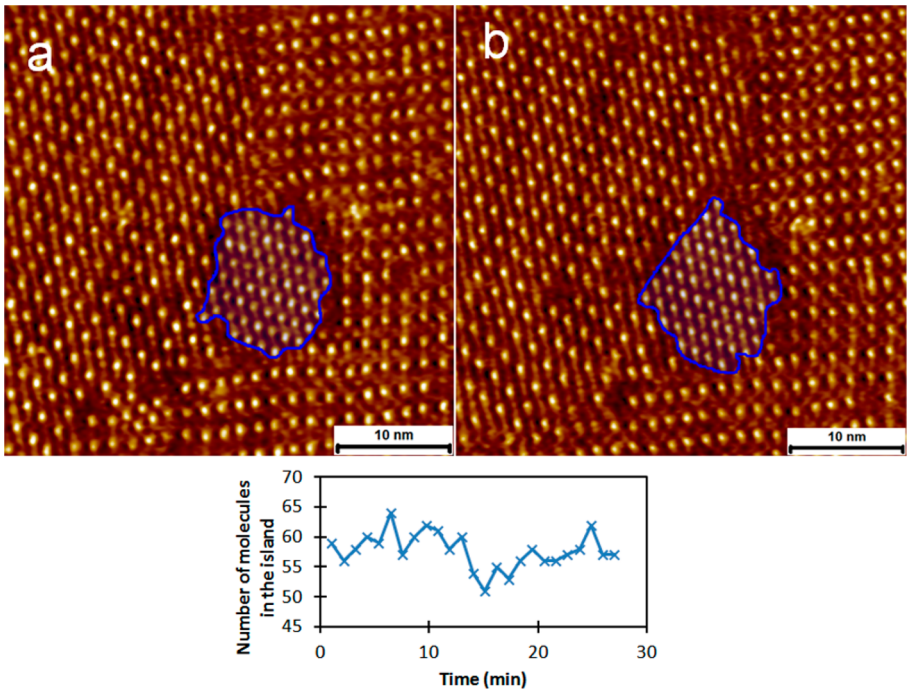

Figure 7. (a,b) Two different STM images taken at 22 °C and separated by a 75 s time interval, of the same CoOEP island. The inset shows fluctuation in the number of molecules inside the CoOEP island located within a 1−1 domain over time. The relative molar concentration is 25:1 coronene/CoOEP.

happen in two ways: the molecules can be exchanged with the supernatant solution or they can migrate from neighboring domains.

To visualize the time dependence of molecular motion on the surface, we first note that changes within islands were very seldom seen. Changes did occur at the boundaries between islands. To better visualize these boundary changes, consider the expanded region around a small CoOEP island shown in Figure 6c,d with a 75 s time laps. Green circles are representative of molecules that have added to the CoOEP island and red circles represent molecules that leave the island. The white circles in Figure 6c,d indicate CoOEP molecules that do not change position and that serve as convenient markers to help identify the CoOEP that joined or departed the island. The yellow marked CoOEPs are representative of newly disordered molecules that belong to neither the CoOEP island nor the surrounding 1−1 grain. The CoOEP islands in both panels c and d are blue-highlighted for easier comparison.

Given the >100 kJ/mol activation energy for desorption of CoOEP,[32] it is unlikely that CoOEP would be lost to solution in the 75 s time interval. On the contrary, porphyrins are quite mobile on clean gold surfaces, so movement from island to disordered to a different island is possible. The desorption energy for coronene is much less than that for CoOEP (vide infra), and desorption of coronene from the disordered edges of islands might occur. This, in turn, could make room for CoOEP. The data presented in Figure 6 does not allow us to definitively say more than that at 22 °C the grain boundaries are not static over short times but the interiors are.

To further investigate dynamic changes in surface coverage at 22 °C, we captured multiple consecutive images to track the number of CoOEP molecules in one CoOEP island. Figure 7a,b shows two sequential images of an island separated in time by 75 s. It is apparent from the change in shape of the island that some movement of molecules is occurring. The plot in the bottom panel of Figure 7 shows the fluctuation in the number of molecules in the small CoOEP domain imbedded in large islands of 1−1 structure over the course of 27 min. This fluctuation about a mean suggests the possibility of equilibrium along the domain boundaries. From these experiments one can postulate that the total number of surface CoOEP is not changing but their distribution between grain boundaries and disorder is fluctuating.

While individual islands appear to be statistically stable for at least hours at 22 °C, this is not the case at 50 °C. As shown in Figure 5, the 1−1 structure is not stable at 50 °C and relaxes into a pure CoOEP covered surface. At this higher temperature nucleation of the oblique CoOEP structure from inside a 1−1 domain occurs and growth of the CoOEP islands can proceed from both the interior and boundaries of islands. STM images showing examples of both processes are presented in Figure S9 in the Supporting Information.

V. COMPUTATIONAL RESULTS AND DISCUSSION

An estimation of the relative adsorption energy is desirable to understand the relative stability of these phases with concentration. We primarily focus on the energy rather than the free energy because these are not equilibrium processes. To determine the binding energies, we have performed periodic DFT calculations on 1−1 CoOEP-coronene/Au(111), on CoOEP/Au(111), on coronene/Au(111), and on isolated coronene and CoOEP molecules. Detailed descriptions of the simulation model and optimizations are presented in the Supporting Information. Note that all calculations performed on various molecules/systems here are done without any explicit or implicit solvation and hence the obtained results are for desorption into vacuum and can be used only for qualitative comparison.

The binding/adsorption energies of different adsorbates are listed in Table 2. It was found that the 1−1 structure binds

DOI: 10.1021/acs.jpcc.5b07120
J. Phys. Chem. C 2015, 119, 25364−25376

Table 2. Calculated Adsorption Energies, Interface Dipole Energies, and Energy per nm^2 for CoOEP, Coronene, and 1:1 CoOEP/Coronene on Au(111) and the Computed Normal Vibration Motion of the Molecule as a Whole Relative to the Surface in UHV[a,b]

adsorbate	substrate	adsorption energy	interface dipole (eV)	energy density	ν_S (cm^{-1})[b]
CoOEP (phase-segregated)	Au(111)	−4.34 eV	0.50	−2.68 eV/nm^2	77
		417 kJ/mol		-4.29×10^{-19} J/nm^2	
Coronene (phase-segregated)	Au(111)	−2.40 eV	0.16	−2.06 eV/nm^2	99
		−231 kJ/mol		-3.30×10^{-19} J/nm^2	
CoOEP/coronene	Au(111)	−7.01 eV	0.71	−2.60 eV/nm^2	
(1−1 structure)		−674 kJ/mol		-4.16×10^{-19} J/nm^2	
CoOEP from 1:1 structure	Au(111)	−4.50 eV			
		−433 kJ/mol			
coronene from 1:1 structure	Au(111)	−2.55 eV			
		−245 kJ/mol			

[a]Energies for the 1−1 structure are either that for the two-component monolayer or for removing all of one type of molecule from the surface while maintaining the other in its original position. See the details in the adsorption energies section in the Supporting Information. [b]Details of vibrational frequency calculation in the Supporting Information (Figures S8 and S9 and text).

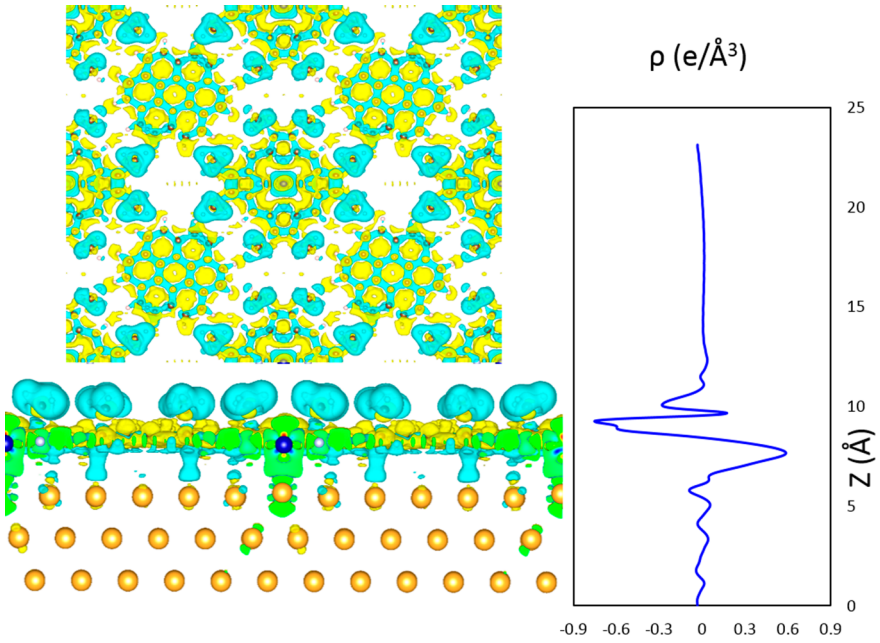

Figure 8. Charge density difference for CoOEP-Coronene/Au(111) system. Figure on the left represents the 3-D iso-density (+ve: yellow and−ve: cyan) of charge density difference. The plot on the right is the x−y plane averaged charge difference, with charge density (ρ) on the x axis and distance (Å) in the z direction of the interface unit cell on the y axis.

(−7.01 eV) slightly more strongly to Au(111) (by 0.27 eV) than the sum of the adsorption energies of CoOEP (−4.34 eV) and coronene (−2.40 eV) by themselves (phase-segregated structures). This difference can be attributed to the combination of intermolecular/packing forces between CoOEP and coronene in the monolayer. In fact, the binding energies of CoOEP and coronene to Au(111) in the 1−1 structure are greater by 0.16 and 0.15 eV, respectively, than their phase-segregated structures (Table 2).

In addition to the binding energies, we were able to obtain the interfacial charge redistribution and interface dipole energies of CoOEP, coronene, and 1−1 structures on Au(111). Charge redistribution or charge density (CD) difference at the adsorbate−adsorbent interface was obtained using Poisson's equation similar to previous studies.[63,75] Note that the charge densities for the adsorbate and adsorbent are obtained from exactly the same geometries as in the adsorbate−adsorbent complex. Three dimensional (3-D) charge redistribution and plane-averaged (ab-plane) CD difference in the z direction for CoOEP−coronene/Au(111) interface are depicted in the left and right panels of Figure 8. Similar CD difference images/plots for phase-segregated CoOEP, coronene systems on Au(111) are depicted in Figure S4.

Examining the 3D images of in Figure 8 (left panel), it can be observed that the most positive charge (yellow color) is centralized on coronene, while the most negative charge (cyan color) is concentrated on the CoOEP structure. This depiction clearly indicates the presence of charge imbalance between coronene and CoOEP in the 1−1 structure. The plane averaged CD difference in the z direction looks similar for both 1−1 (right panel Figure 8) and phase segregated (Figure S4) structures, but the amount of charge is varied as depicted in y-axis values in each case. Additionally the interface dipole energies also vary significantly in each system, as shown in Table 2. Interface dipole energies are obtained by numerically integrating the (1-D) Poisson equation (i.e., electrostatic

DOI: 10.1021/acs.jpcc.5b07120
J. Phys. Chem. C 2015, 119, 25364−25376

potential energy difference between monolayers (coronene, CoOEP, or 1−1 structure) and Au(111) surface), as was performed in similar previous studies.[76] CoOEP (phase-segregated) exhibits a larger surface dipole than does coronene (phase segregated). Also interestingly, the interface dipole energy in the 1−1 CoOEP−coronene structure (0.71 eV) appears to be approximately equal to the sum of the dipoles (0.56 + 0.16 eV) in phase-segregated systems. The above findings clearly demonstrate the role of van der Waals, dipole, and packing forces in the formation of the 1−1 structure.

The energy of CoOEP and of coronene on gold was computed as a function of the distance between the rigid molecule and the gold surface. These computations were performed using the optimized geometries of CoOEP and of coronene on Au(111) as reference. The obtained potentials were fit to a polynomial curve, and the quadratic term was used to extract a force constant. That force constant and the mass of the molecule were used to compute an effective surface normal vibrations, ν_S. Values for ν_S are included in Table 2.

UHV studies show that ethyl groups of NiOEP molecules adsorbed on Au(111) are standing upward and normal to the surface.[71] This configuration is also consistent with the CoOEP−CoOEP and CoOEP−coronene distances observed experimentally. Hence it is the presumed configuration for CoOEP on Au(111), and this configuration has been used throughout all of our calculations. A 3D model of the 1−1 structure based on the STM images (Figure S2) suggests that the coronene molecule is sterically hindered from desorption by the eight ethyl groups of surrounding CoOEP molecules. This may play a key role in allowing this structure to be kinetically favored over a relatively large concentration range of excess coronene.

To better understand the energetics of the various phases, a useful quantity is the adsorption energy per unit area. This is the appropriate quantity because the coverage per molecule of each phase is different. Using the actual experimental unit cells reported in Figure 1 and the computed energy of adsorption in UHV, the energy/nm^2 for each phase is estimated in Table 2. Surprisingly, the energy produced by the formation of a unit area of the 1−1 structure is only slightly less than that for pure CoOEP but much more than that for the same area covered by coronene. It is most useful to view these energies as estimates for the energy of activation for desorption of coronene or CoOEP. Thus, at low temperatures and in the absence of activation barriers a pure CoOEP monolayer would always be both energetically preferred and the kinetically most stable as long as there existed sufficient CoOEP in solution to form a complete monolayer. The second most stable structure would be the 1−1 structure, and the coronene monolayer would be the least stable.

VI. GENERAL RESULTS AND DISCUSSION

Before proceeding to discuss the kinetic implications, it is worthwhile to address the issue of desorption energies in solution versus calculated values in UHV. To good approximation one may write[77]

$$\Delta E^1 = -\Delta E_{sub} + \Delta E + \Delta E_{sol} + \Delta E_{wet} \quad (1)$$

where ΔE^1 is the energy of desorption from gold into phenyloctane, ΔE_{sub} is the energy of sublimation, ΔE is the energy of desorption from gold into UHV, ΔE_{sol} is the energy change when crystalline solid dissolves in phenyloctane, and ΔE_{wet} is the energy associated with the difference in wetting a gold surface and a molecule covered gold surface with phenyloctane. We show in Table S3 that the DFT-calculated desorption energies are too large but that the trend (desorption energy of coronene much less than of CoOEP) is correct.

Given that the activation energy for desorption of coronene from gold into phenyloctane is much less than for CoOEP in the same process, it is expected that coronene (in a pure monolayer) will exchange with coronene in solution at temperatures where CoOEP will not. This is clearly the case, as is demonstrated by the rapid conversion of a prepared monolayer of coronene to either one of the CoOEPs or to the 1−1 structure upon exposure to a solution containing sufficient CoOEP to compete with coronene for adsorption sites. Similarly, the ability to convert the 1−1 structure to a pure CoOEP surface (but not go the other way) with exposure to an appropriate concentration solution clearly shows that the coronene in the 1−1 structure is still capable of desorption from the surface. Furthermore, as previously mentioned, the CoOEP desorption rate at 22 °C is essentially zero on the time scale of these experiments. Thus, it is our conclusion that these structures are forming at the nucleation stage and then growing faster than the others because of a combination of impingement and desorption rates.

The impingement rates depend on the diffusion coefficients and the concentrations of each component in solution. The diffusion coefficients for coronene and CoOEP in phenyloctane can be estimated using the Stokes−Einstein equation—either for our disk-like molecules based on our computed molecular sizes[78] or by using the crystallographically determined molecular volumes. Either method yields similar results. The diffusion coefficient for coronene in phenyloctane at 22 °C is $\sim 2.0 \times 10^{-10}$ m^2/s, while that for CoOEP is $\sim 1.5 \times 10^{-10}$ m^2/s. Thus, even in the case of equal concentrations of coronene and CoOEP, the coronene is hitting the surface somewhat faster than CoOEP. At the very high coronene/CoOEP ratios important to the observed surface composition change, the impingement rates for coronene are one to two orders of magnitude higher than for CoOEP. Because the desorption rate of CoOEP is many orders slower than for coronene, it requires large excesses of coronene in solution (and therefore impingement rates) for either the 1−1 or pure coronene structure to grow sufficiently fast to inhibit the growth of the CoOEP monolayer.

If one wanted to apply a thermodynamic argument (which we believe is not appropriate here) it is necessary to determine the relative free energies, and for these the entropies of adsorption must be considered. The translational and rotational entropy for each solute can be estimated using a model first proposed by Whitesides[79] and recently used by Lackinger.[77] The entropy associated with the normal surface vibrational mode of the bound adsorbate was estimated using the frequencies in Table 2. Typical values were also selected for the other five rigid body motions of the adsorbed molecules. Thus, for a 1×10^{-4} M solution of CoOEP in octylbenzene one find $\Delta S_{ads} = -280$ J/(mol K). For coronene, the same calculation yields $\Delta S_{ads} = -260$ J/(mol K). Furthermore, these values are only weakly dependent on solution concentration. At 298 K, the difference in the $T\Delta S_{ads}$ terms is only 0.07 eV per molecule. Therefore, in the absence of differences in solvent coadsorption, the entropic term will not have a significant effect on the relative free energies of adsorption. We reiterate, however, our belief that this process is kinetically controlled.

DOI: 10.1021/acs.jpcc.5b07120
J. Phys. Chem. C 2015, 119, 25364−25376

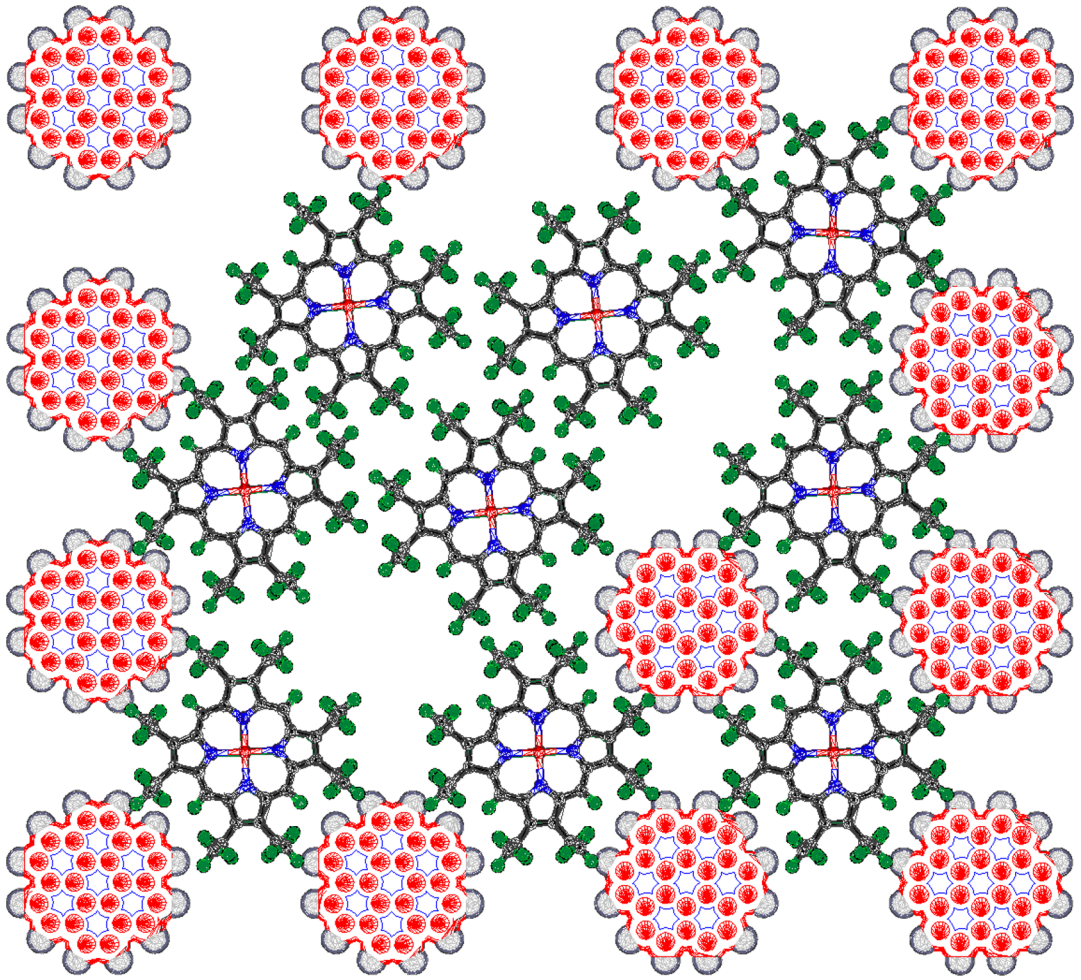

Figure 9. Representation of nucleation of CoOEP structure in a 1−1 island requiring desorption of three coronene molecules and rearrangement of four nearest CoOEPs.

This is a really key point. Equilibrium is about rates at steady state where all species are freely exchanging. Thus, the chemical potential in solution of each species may be directly related to the chemical potential of the related species (or perhaps compound) on the surface. In this work, at 22 °C, one of the components, CoOEP, does not desorb (the rate of desorption from HOPG is faster than from Au(111) and that rate constant is 1.0/year![80]) so there is no way to establish equilibrium. The rate constants related to phase formation in this case are NOT the steady state rates, but rather the rates of initial adsorption and desorption on a clean gold surface. For these mixtures at room temperature, CoOEP molecules that stick to the gold surface never come off, but the coronene is able to exchange with the solution. Thus, the real question is "So long as there is enough CoOEP in solution to make a monolayer (there was in these experiments) why isn't a CoOEP monolayer always formed ?"

These observations about relative rates do create a concern. If the coronene is labile and the CoOEP is not, why is the 1−1 structure not spontaneously changing to the lower energy and more kinetically stable CoOEP monolayer? While this may in fact be occurring extremely slowly at room temperature, the time scale is still vastly longer than the conversion from a pure coronene surface to either the 1−1 or pure CoOEP structure. Furthermore, any such change at room temperature is primarily occurring at the grain boundaries. The stability of the 1−1 phase can be possible if the rate of desorption of a single coronene from the 1−1 structure is much slower than from pure coronene or if it requires the cooperative action of other molecules. While the computed desorption energy for coronene in the 1−1 structure is greater than that for the pure coronene layer—and therefore the rate decreases because of the Arrhenius activation energy increase—we think that change is insufficient to account for the stability of the 1−1 phase. An additional decrease in desorption rate created by the steric hindrance afforded by the surrounding ethyl groups probably further reduces the desorption rate for coronene in the 1−1 structure; however, we believe that neither of these effects is sufficient. We attribute the long-term stability of the 1−1 structure to the kinetic problem of nucleating the CoOEP phase within the 1−1 structure.

Consider Figure 9. In this Figure we have removed three adjacent coronene molecules from the 1−1 unit-cell structure and rearranged four nearest neighbor CoOEP into the CoOEP monolayer structure. Note that removal of three coronene molecules allows only rearrangement of CoOEP molecules to nucleate, but no additional CoOEP molecules can be added from supernatant solution onto the surface. Because coronene is much smaller than CoOEP, removing fewer than three does not provide sufficient continuous space either for adsorption of a CoOEP or for nucleation. Thus, the essential event required for conversion within a grain is a very low probability event—

DOI: 10.1021/acs.jpcc.5b07120
J. Phys. Chem. C 2015, 119, 25364−25376

three coronenes surrounding a particular CoOEP must all be desorbed before one of them is replaced by a coronene from solution.

A referee has pointed out that this need for nearly simultaneous desorption of several coronenes used for the 1−1 to pure CoOEP structure conversion can also account for the sharp transition from pure coronene to 1−1 structure. Three adjacent coronene molecules must be gone from the coronene monolayer to allow a single CoOEP to adsorb. As long as the coronene impingement rate is much higher than that of CoOEP (much higher concentration), this is a very improbable event.

VII. CONCLUSIONS

Three different surface structures can be formed from a mixed solution of coronene and CoOEP at the phenyloctane/Au(111) interface depending on the relative molar concentration of two components. These structures consist of the pure CoOEP monolayer structure, the pure coronene monolayer structure, and a 2-D cocrystal of coronene and CoOEP. An oblique unit cell for CoOEP was defined that consists of one molecule of CoOEP. Lattice parameters of the CoOEP structure were determined to be A = (1.46 ± 0.04) nm, B = (1.34 ± 0.04) nm, and α = 56° ± 2°. Bhattarai et al.[32] reported the lattice parameters of CoOEP at the phenylocatane/Au(111) interface to be A = (1.42 ± 0.02) nm, B = (1.32 ± 0.02) nm, and α = 57 ± 2°, which agree with ours within experimental error. The unit cell of coronene was found to be hexagonal with lattice parameters, A = B = (1.16 ± 0.04) nm. Previously we reported the unit cell of the dense hexagonal structure of coronene at the heptanoic acid/Au(111) interface to be A = B = (1.19 ± 0.04) nm.[72] Unit-cell parameters for the new cocrystal structure were found to be A = (1.73 ± 0.04) nm, B = (1.56 ± 0.04) nm, and α = 90 ± 2°. Two sharp transitions in structure, one from CoOEP structure to cocrystal structure and a second from cocrystal structure to coronene, were observed upon increasing the amount of coronene in the mixed supernatant solutions. It was possible to convert the pure coronene structure to either the 1−1 or CoOEP structure and the 1−1 structure to CoOEP, but the reverse transformations were never observed.

Periodic DFT calculations of nonsolvated CoOEP, coronene and 1−1 CoOEP−coronene structures on the Au(111) surface revealed that CoOEP binds more strongly to Au(111) than coronene. Also, the selective desorption energies of CoOEP or coronene from the 1−1 structure on Au(111) are slightly higher than the respective desorption energies when obtained from individually simulated CoOEP/Au(111) and coronene/Au(111) systems. This difference indicates the presence of additional intermolecular forces in the 1−1 structure. Furthermore, experiments based on the relative adsorption strength along with in situ heating experiments showed that the pure CoOEP structure is stable on the surface while the new cocrystal structure was kinetically trapped. We attribute the 22 °C longevity of the 1−1 structure to a combination of factors including decreased rate of desorption for an individual coronene and the need for simultaneous desorption of three coronenes surrounding a CoOEP to nucleate the CoOEP phase. Time-dependent STM imaging illustrated the exchange of molecules at grain boundaries at 22 °C and the nucleation and growth of pure CoOEP monolayer at 50 °C.

This system is unusual in many ways, but the absence of any significant lateral forces other than van der Waals and steric constraints is notable. Also notable is the fact that the construction of the well-ordered 1−1 adlayer requires that the components have solution concentrations differing by a factor of >10. A critical element is the fact that one component (CoOEP) is irreversibly adsorbed. By demonstrating that novel structures can be formed from solutions with component concentrations an order of magnitude different than the surface concentration, we hope to stimulate the development of new self-assembled structures through the use of conditions far from those frequently utilized.

■ ASSOCIATED CONTENT

Supporting Information

The Supporting Information is available free of charge on the ACS Publications website at DOI: 10.1021/acs.jpcc.5b07120.

Solvent purification procedure, STM images of surface structures at different molar ratios of coronene/CoOEP on Au(111), entrapment of coronene molecules by ethyl substituents of CoOEP in 1−1 structure, simulation model, calculation of absorption energies and surface normal vibrational frequencies, conversion mechanisms of 1−1 structure to CoOEP structure, and the procedure for measuring heats of solution of CoOEP and coronene in phenyloctane. (PDF)

■ AUTHOR INFORMATION

Corresponding Author

*E-mail: hipps@wsu.edu. Tel: (509) 335-3033.

Notes

The authors declare no competing financial interest.

■ ACKNOWLEDGMENTS

This material is based on work supported by the National Science Foundation under Grants CHE-1403989 and CHE-1112156. The computational work was performed using EMSL, a DOE Office of Science User Facility sponsored by the Office of Biological and Environmental Research and located at Pacific Northwest National Laboratory (PNNL). Part of the computations were also supported by resources from PNNL Institutional Computing (PIC) program at PNNL.

■ REFERENCES

(1) Khassanov, A.; Steinrueck, H.-G.; Schmaltz, T.; Magerl, A.; Halik, M. Structural Investigations of Self-Assembled Monolayers for Organic Electronics: Results from X-ray Reflectivity. *Acc. Chem. Res.* **2015**, *48*, 1901.

(2) Sakamoto, R.; Iwashima, T.; Tsuchiya, M.; Toyoda, R.; Matsuoka, R.; Kogel, J. F.; Kusaka, S.; Hoshiko, K.; Yagi, T.; Nagayama, T.; Nishihara, H. New Aspects in bis and tris(dipyrrinato) metal Complexes: Bright Luminescence, Self-assembled Nanoarchitectures, and Materials Applications. *J. Mater. Chem. A* **2015**, *3*, 15357 http://pubs.rsc.org/en/content/articlepdf/2015/ta/c5ta02040a,.

(3) Yang, Y.; Sun, Y.; Song, N. Switchable Host-Guest Systems on Surfaces. *Acc. Chem. Res.* **2014**, *47*, 1950−1960.

(4) Muller, T. STEM: Self-Assembly on Graphite. In *Dekker Encyclopedia of Nanoscience and Nanotechnology*, 3rd ed.; Taylor & Francis: New York, 2014; pp 4653−4662.

(5) Onodera, T.; Toko, K. Towards an Electronic Dog Nose: Surface Plasmon Resonance Immunosensor for Security and Safety. *Sensors* **2014**, *14*, 16586−16616.

(6) Ko, S.; Han, G.; Lee, J. K. Surface Organic Chemistry for Application to Organic Electronics. *Tetrahedron Lett.* **2015**, *56*, 3721−3731.

(7) Stadler, C.; Hansen, S.; Kroger, I.; Kumpf, C.; Umbach, E. Tuning Intermolecular Interaction in Long-Range-Ordered Submonolayer Organic Films. *Nat. Phys.* **2009**, *5*, 153−158.
(8) Mali, K. S.; Van Averbeke, B.; Bhinde, T.; Brewer, A. Y.; Arnold, T.; Lazzaroni, R.; Clarke, S. M.; De Feyter, S. To Mix or Not to Mix, 2D Crystallization and Mixing Behavior of Saturated and Unsaturated Aliphatic Primary Amides. *ACS Nano* **2011**, *5*, 9122−9137.
(9) Mali, K. S.; Lava, K.; Binnemans, K.; De feyter, S. Hydrogen Bonding versus van der Waals Interactions: Competetive Influence of Noncovalent Interactions on 2D Self-Assembly at the Liquid-Solid Interface. *Chem. - Eur. J.* **2010**, *16*, 14447−14458.
(10) Gutzler, R.; Sirtl, T.; Dienstmaier, J. F.; Mahata, K.; Heckl, W. M.; Schmittel, M.; Lackinger, M. Reversible Phase Transition in Self-Assembled Monolayers at the Liquid-Solid Interface: Temperature-Controlled Opening and Closing of Nanopores. *J. Am. Chem. Soc.* **2010**, *132*, 5084−5090.
(11) Gao, Y.; Zhang, X.; Ma, C.; Li, X.; Jiang, J. Morphology-Controlled Self-Assembled Nanostructures of 5,15-Di[4-(5 acetylsulfanylpentyloxy)phenyl]porphyrin Derivatives. Effect of Metal-Ligand Coordination Bonding on Tuning the Intermolecular Interaction. *J. Am. Chem. Soc.* **2008**, *130*, 17044−17052.
(12) Kim, M. K.; Xue, Y.; Paskova, T.; Zimmt, M. Monolayer Pattering using Ketone Dipoles. *Phys. Chem. Chem. Phys.* **2013**, *15*, 12466−12474.
(13) Hipps, K. W.; Scudiero, L.; Barlow, D. E.; Cooke, M. P.; Self-Organized, A. 2-Dimensional Bifunctional Structure Formed by Supramolecular Design. *J. Am. Chem. Soc.* **2002**, *124*, 2126−2127.
(14) Scudiero, L.; Barlow, D. E.; Hipps, K. W. A Self-Organized Two-Dimensional Bimolecular Structure. *J. Phys. Chem. B* **2003**, *107*, 2903−2909.
(15) Barth, J. V. Fresh Perspectives for Surface Coordination Chemistry. *Surf. Sci.* **2009**, *603*, 1533−1541.
(16) Stadtmuller, B.; Luftner, D.; Willenbockel, M.; Reinisch, E.; Sueyoshi, T.; Koller, G.; Soubatch, S.; Ramsey, M.; Puschnig, P.; Tautz, S.; Kumpf, C. Unexpected Interplay of Bonding Height and Energy Level Alignment at Heteromolecular Hybrid Interfaces. *Nat. Commun.* **2014**, *5*, 3685.
(17) Dmitriev, A.; Spillmann, H.; Lin, N.; Barth, J.; Kern, K. Modular Assembly of Two-Dimensional Metal−Organic Coordination Networks at a Metal Surface. *Angew. Chem., Int. Ed.* **2003**, *42*, 2670−2673.
(18) Barrena, E.; de Oteyza, D. G.; Dosch, H.; Wakayama, Y. 2D Supramolecular Self-Assembly of Binary Organic Monolayers. *ChemPhysChem* **2007**, *8*, 1915−1918.
(19) MacLeod, J. M.; Ivasenko, O.; Perepichka, D. F.; Rosei, F. Stabilization of Exotic Minority Phases in a Multicomponent Self-Assembled Molecular Network. *Nanotechnology* **2007**, *18*, 424031/1−424031/9.
(20) Yoshimoto, S.; Honda, Y.; Ito, O.; Itaya, K. Supramolecular Pattern of Fullerene on 2D Bimolecular "Chessboard" Consisting of Bottom-up Assembly of Porphyrin and Phthalocyanine Molecules. *J. Am. Chem. Soc.* **2008**, *130*, 1085−1092.
(21) Griessl, S.; Lackinger, M.; Edelwirth, M.; Hietschold, M.; Heckl, W. M. Self-Assembled Two-Dimensional Molecular Host-Guest Architectures From Trimesic Acid. *Single Mol.* **2002**, *3*, 25−31.
(22) Wei, Y.; Tong, W.; Zimmt, M. J. Self-Assembly of Patterned Monolayers with Nanometer Features: Molecular Selection Based on Dipole Interactions and Chain Length. *J. Am. Chem. Soc.* **2008**, *130*, 3399−3405.
(23) Nath, K. G.; Ivasenko, O.; Miwa, J. A.; Dang, H.; Wuest, J. D.; Nanci, A.; Perepichka, D. F.; Rosei, F. Rational Modulation of the Periodicity in Linear Hydrogen-Bonded Assemblies of Trimesic Acid on Surfaces. *J. Am. Chem. Soc.* **2006**, *128*, 4212−4213.
(24) Gyarfas, B.; Wiggins, B.; Zosel, M.; Hipps, K. W. Supramolecular Structures of Coronene and Alkane Acids at the Au(111)-Solution Interface: A Scanning Tunneling Microscopy Study. *Langmuir* **2005**, *21*, 919−923.
(25) Yang, Y.; Wang, C. Solvent Effects on Two-Dimensional Molecular Self-Assemblies Investigated by Using Scanning Tunneling Microscopy. *Curr. Opin. Colloid Interface Sci.* **2009**, *14*, 135−147.
(26) Mamdouh, W.; Uji-I, H.; Ladislaw, J.; Dulcey, A.; Percec, V.; De Schryver, F.; De Feyter, S. Solvent Controlled Self-Assembly at the Liquid/Solid Interface Revealed by STM. *J. Am. Chem. Soc.* **2006**, *128*, 317−325.
(27) Kampschulte, L.; Lackinger, M.; Maier, A.-K.; Kishore, R. S. K.; Griessl, S.; Schmittel, M.; Heckl, W. Solvent Induced Polymorphism in Supramolecular 1,3,5-Benzenetribenzoic Acid Monolayers. *J. Phys. Chem. B* **2006**, *110*, 10829−10836.
(28) Shimon, L. J. W.; Vaida, M.; Addadi, L.; Lahav, M.; Leiserowitz, L. Molecular Recognition at the Solid-Solution Interface: A "Relay" Mechanism for the Effect of Solvent on Crystal Growth and Dissolution. *J. Am. Chem. Soc.* **1990**, *112*, 6215−6220.
(29) Venkataraman, B.; Breen, J. J.; Flynn, G. W. Scanning Tunneling Microscopy Studies of Solvent Effects on the Adsorption and Mobility of Triacontane/Triacontanol Molecules Adsorbed on Graphite. *J. Phys. Chem.* **1995**, *99*, 6608−6619.
(30) Yang, Z.-Y.; Lei, S.-B.; Gan, L.-H.; Wan, L.-J.; Wang, C.; Bai, C.-L. The Effect of Polarity on Co-Adsorbed Molecular Nanostructure with Substituted Phthalocyanine and Thiol Molecules. *ChemPhysChem* **2005**, *6*, 65−70.
(31) Castro, M. A.; Clarke, S. M.; Inaba, A.; Thomas, R.; Arnold, T. Preferential Adsorption from Binary Mixtures of Short Chain n-Alkanes; The Octane-Decane System. *J. Phys. Chem. B* **2001**, *105*, 8577−8582.
(32) Bhattarai, A.; Mazur, U.; Hipps, K. W. A Single Molecule Level Study of the Temperature Dependent Kinetics for the Formation of Metal Porphyrin Monolayers on Au(111) from Solution. *J. Am. Chem. Soc.* **2014**, *136*, 2142−2148.
(33) Bhattarai, A.; Mazur, U.; Hipps, K. W. Desorption Kinetics and Activation Energy for Cobalt Octaethylporphyrin from Graphite at the Phenyloctane Solution−Graphite Interface: An STM Study. *J. Phys. Chem. C* **2015**, *119*, 9386−9394.
(34) Ikeda, T.; Asakawa, M.; Goto, M.; Miyake, K.; Ishida, T.; Shimizu, T. STM Observation of Alkane-assisted Self-assembled Monolayers of Pyridine-coordinated Porphyrin Rhodium Chlorides. *Langmuir* **2004**, *20*, 5454−5459.
(35) Yablon, D. G.; Ertas, D.; Fang, H.; Flynn, G. W. An STM Investigation of the Adsorption of Mixtures of Fatty Acids and Substituted Acids at the Solution-Graphite Interface. *Isr. J. Chem.* **2003**, *43*, 383−392.
(36) Yoshimoto, S.; Higa, N.; Itaya, K. Two-Dimensional Supramolecular Organization of Copper Octaethylporphyrin and Cobalt Phthalocyanine on Au(111): Molecular Assembly Control at an Electrochemical Interface. *J. Am. Chem. Soc.* **2004**, *126*, 8540−8545.
(37) Stevens, F.; Beebe, T. P. Dynamical Exchange Behavior in Organic Monolayers Studied by STM Analysis of Labeled Mixtures. *Langmuir* **1999**, *15*, 6884−6889.
(38) Kampschulte, L.; Werblowsky, T. L.; Kishore, R. S. K.; Schmittel, M.; Heckl, W. M.; Lackinger, M. Thermodynamical Equilibrium of Binary Supramolecular Networks at the Liquid-Solid Interface. *J. Am. Chem. Soc.* **2008**, *130*, 8502−8507.
(39) Eder, G.; Kloft, S.; Martsinovich, N.; Mahata, K.; Schmittel, M.; Heckl, W. M.; Lackinger, M. Incorporation Dynamics of Molecular Guests into Two-Dimensional Supramolecular Host Networks at the Liquid Solid Interface. *Langmuir* **2011**, *27*, 13563−13571.
(40) Griessl, S.; Lackinger, M.; Jamitzky, F.; Markert, T.; Hietschold, M.; Heckl, W. Incorporation and Manipulation of Coronene in an Organic Template Structure - Single Molecular Rotation. *Langmuir* **2004**, *20*, 9403−9407.
(41) Lei, S.; Surin, M.; Tahara, K.; Adisoejoso, J.; Lazzaroni, R.; Tobe, Y.; Feyter, S. D. Programmable Hierarchical Three-Component 2D Assembly at a Liquid-Solid interface: Recognition, Selection and Transformation. *Nano Lett.* **2008**, *8*, 2541−2546.
(42) Schull, G.; Douillard, L.; Fiorini-Debuisschert, C.; Charra, F.; Mathevet, F.; Kreher, D.; Attias, A.-J. Single-Molecule Dynamics in a Self-Assembled 2D Molecular Sieve. *Nano Lett.* **2006**, *6*, 1360−1363.
(43) Ivasenko, O.; MacLeod, J. M.; Chernichenko, K. Y.; Balenkova, E. S.; Shpanchenko, R. V.; Nenajdenko, V. G.; Rosei, F.; Perepichka,

DOI: 10.1021/acs.jpcc.5b07120
J. Phys. Chem. C 2015, 119, 25364−25376

D. F. Supramolecular Assembly of Heterocirculenes in 2D and 3D. *Chem. Commun.* **2009**, *10*, 1192−1194.
(44) Wei, X.; Tong, W.; Fidler, V.; Zimmt, M. B. Reactive Capture of Gold Nanoparticles by Strongly Physisorbed Monolayers on Graphite. *J. Colloid Interface Sci.* **2012**, *387*, 221−227.
(45) Zou, Z.; Wei, L.; Chen, F.; Liu, Z.; Thamyongkit, P.; Loewe, R. S.; Lindsey, J. S.; Mohideen, U.; Bocian, D. J. Solution STM Images of Porphyrins on HOPG reveal that Subtle Differences in Molecular Structure Dramatically Alter Packing Geometry. *J. Porphyrins Phthalocyanines* **2005**, *9*, 387−392.
(46) Yoshimoto, S.; Honda, Y.; Ito, O.; Itaya, K. Supramolecular Pattern of Fullerene on 2D Bimolecular "Chessboard" Consisting of Bottom-up Assembly of Porphyrin and Phthalocyanine Molecules. *J. Am. Chem. Soc.* **2008**, *130*, 1085−1092.
(47) Mazur, U.; Hipps, K. W. Kinetic and Thermodynamic Processes of Organic Species at the Solution-Solid Interface: the View Through an STM. *Chem. Commun.* **2015**, *51*, 4737−4749.
(48) Friesen, B. A.; Bhattarai, A.; Mazur, U.; Hipps, K. W. Single Molecule Imaging of Oxygenation of Cobalt Octaethylporphyrin at the Solution/Solid Interface: Thermodynamics from Microscopy. *J. Am. Chem. Soc.* **2012**, *134*, 14897−14904.
(49) Stevens, F.; Beebe, T. P. Dynamical Exchange Behavior in Organic Monolayers Studied by STM Analysis of Labeled Mixtures. *Langmuir* **1999**, *15*, 6884−6889.
(50) Blunt, M. O.; Adisoejoso, J.; Tahara, K.; Katayama, K.; Van der Auweraer, M.; Tobe, Y.; De feyter, S. Temperature-induced Structural Phase Transition in a Two-Dimensional Self-Assembled Network. *J. Am. Chem. Soc.* **2013**, *135*, 12068−12075.
(51) Lu, X.; Hipps, K. W. Scanning Tunneling Microscopy of Metal Phthalocyanines: d^6 and d^8 Cases. *J. Phys. Chem. B* **1997**, *101*, 5391−5396.
(52) Lu, X.; Hipps, K. W.; Wang, X.; Mazur, U. Scanning Tunneling Microscopy of Metal Phthalocyanines: d^7 and d^9 Cases. *J. Am. Chem. Soc.* **1996**, *118*, 7197−7202.
(53) Barlow, D.; Hipps, K. W. A Scanning Tunneling Microscopy and Spectroscopy Study of Vanadyl Phthalocyanine on Au(111): the Effect of Oxygen Binding and Orbital Mediated Tunneling on the Apparent Corrugation. *J. Phys. Chem. B* **2000**, *104*, 5993−6000.
(54) Jahanbekam, A.; Mazur, U.; Hipps, K. W. A New Variable Temperature STM For the solution solid interface. *Rev. Sci. Instrum.* **2014**, *85*, 103701−103706.
(55) SPIP is a product of Image Metrology, Lyngsø Alle 3A, DK-2970 Hørsholm, Denmark.
(56) Tong, W.; Xue, Y.; Zimmt, M. B. Morphology Control and Monolayer Patterning with CF2 Groups: An STM Study. *J. Phys. Chem. C* **2010**, *114*, 20783−20792.
(57) Tong, W. Controlling Self-Assembled Monolayer Morphology with Dipolar Interactions: Preparation, STM Image Analysis and Simulations of 1,5-(Disubstituted)-anthracene Monolayers. Ph.D. Thesis, Brown University, Providence, RI, 2010.
(58) Kresse, G.; Furthmüller, J. Efficiency of ab-initio Total Energy Calculations for Metals and Semiconductors Using a Plane-Wave Basis Set. *Comput. Mater. Sci.* **1996**, *6*, 15−50.
(59) Kresse, G.; Furthmüller, J. Efficient Iterative Schemes for *ab initio* Total-Energy Calculations Using a Plane-Wave Basis Set. *Phys. Rev. B: Condens. Matter Mater. Phys.* **1996**, *54*, 11169−11186.
(60) Kresse, G.; Hafner, J. Ab initio Molecular Dynamics for Liquid Metals. *Phys. Rev. B: Condens. Matter Mater. Phys.* **1993**, *47*, 558−561.
(61) Kresse, G.; Joubert, D. From Ultrasoft Pseudopotentials to the Projector Augmented-Wave Method. *Phys. Rev. B: Condens. Matter Mater. Phys.* **1999**, *59*, 1758−1775.
(62) Blöchl, P. E. Projector Augmented-Wave Method. *Phys. Rev. B: Condens. Matter Mater. Phys.* **1994**, *50*, 17953−17979.
(63) Chilukuri, B.; Mazur, U.; Hipps, K. W. Effect of Dispersion on Surface Interactions of Cobalt(II) Octaethylporphyrin Monolayer on Au(111) and HOPG(0001) Substrates: A Comparative First Principles Study. *Phys. Chem. Chem. Phys.* **2014**, *16*, 14096−14107.
(64) Klimeš, J.; Bowler, D. R.; Michaelides, A. Van der Waals Density Functionals Applied to Solids. *Phys. Rev. B: Condens. Matter Mater. Phys.* **2011**, *83*, 195131−195131.
(65) Klimeš, J.; Bowler, D. R.; Michaelides, A. Chemical Accuracy for the van der Waals Density Functional. *J. Phys.: Condens. Matter* **2010**, *22*, 022201−5.
(66) Lee, K.; Murray, É. D.; Kong, L.; Lundqvist, B. I.; Langreth, D. C. Higher-Accuracy van der Waals Density Functional. *Phys. Rev. B: Condens. Matter Mater. Phys.* **2010**, *82*, 081101−4.
(67) Lide, D. R. *CRC Handbook of Chemistry and Physics*; 89th ed.. CRC Press: Boca Raton, FL, 2008; pp 12−114.
(68) Monkhorst, H. J.; Pack, J. D. Special points for Brillouin-Zone Integrations. *Phys. Rev. B* **1976**, *13*, 5188−5192.
(69) Barlow, D. E.; Scudiero, L.; Hipps, K. W. Scanning Tunneling Microscopy Study of the Structure and Orbital-Mediated Tunneling Spectra of Cobalt(II) Phthalocyanine and Cobalt(II) Tetraphenylporphyrin on Au(111): Mixed Composition Films. *Langmuir* **2004**, *20*, 4413−4421.
(70) Scudiero, L.; Barlow, D. E.; Mazur, U.; Hipps, K. W. Scanning Tunneling Microscopy, Orbital-Mediated Tunneling Spectroscopy, and Ultraviolet Photoelectron Spectroscopy of Metal(II) Tetraphenylporphyrins Deposited from Vapor. *J. Am. Chem. Soc.* **2001**, *123*, 4073−4080.
(71) Scudiero, L.; Barlow, D. E.; Hipps, K. W. Scanning Tunneling Microscopy, Orbital-Mediated Tunneling Spectroscopy, and Ultraviolet Photoelectron Spectroscopy of Nickel(II) Octaethylporphyrin Deposited from Vapor. *J. Phys. Chem. B* **2002**, *106*, 996−1003.
(72) Jahanbekam, A.; Vorpahl, S.; Mazur, U.; Hipps, K. W. Temperature Stability of Three Commensurate Surface Structures of Coronene Adsorbed on Au(111) from Heptanoic Acid in the 0 to 60 °C Range. *J. Phys. Chem. C* **2013**, *117*, 2914−2919.
(73) English, W. A.; Hipps, K. W. Stability of a Surface Adlayer at Elevated Temperature: Coronene and Heptanoic Acid on Au(111). *J. Phys. Chem. C* **2008**, *112*, 2026−2031.
(74) Yoshimoto, S.; Higa, N.; Itaya, K. Two-Dimensional Supramolecular Organization of Copper Octaethylporphyrin and Cobalt Phthalocyanine on Au(111): Molecular Assembly Control at an Electrochemical Interface. *J. Am. Chem. Soc.* **2004**, *126*, 8540−8545.
(75) Chilukuri, B.; Cundari, T. R. Surface Interactions of Au(I) Cyclo-Trimer with Au(111) and Al(111) Surfaces: A Computational Study. *Surf. Sci.* **2012**, *606*, 1100−1107.
(76) Heimel, G.; Romaner, L.; Brédas, J.-L.; Zojer, E. Organic/Metal Interfaces in Self-Assembled Monolayers of Conjugated Thiols: A First-Principles Benchmark Study. *Surf. Sci.* **2006**, *600*, 4548−4562.
(77) Song, W.; Martsinovich, N.; Heckl, W. M.; Lackinger, M. Born-Haber Cycle for Monolayer Self-Assembly at the Liquid-Solid Interface: Assessing the Enthalpic Driving Force. *J. Am. Chem. Soc.* **2013**, *135*, 14854−14862.
(78) Da Costa, V.; Ribeiro, A.; Sobral, A.; Lobo, V.; Annunziata, O.; Santos, C.; Willis, S.; Price, W.; Esteso, M. Mutual and Self-Diffusion of Charged Porphyrines in Aqueous Solutions. *J. Chem. Thermodyn.* **2012**, *47*, 312−319.
(79) Mammen, M.; Shakhnovich, E.; Deutch, J.; Whitesides, G. M. Estimating the Entropic Cost of Self-Assembly of Multiparticle Hydrogen-Bonded Aggregates Based on the Cyanuric Acid-Melamine Lattice. *J. Org. Chem.* **1998**, *63*, 3821−3830.
(80) This is based on the Arrhenius fit for the desorption energy given in ref 33 and using their reported k_0 value of 3.7×10^{12}/min and activation energy of 103 kJ/mol.

DOI: 10.1021/acs.jpcc.5b07120
J. Phys. Chem. C 2015, 119, 25364−25376